

Sparse feature selection methods identify unexpected global cellular response to strontium-containing materials

Hélène Autefage^{a,b,c}, Eileen Gentleman^{a,b,c,d}, Elena Littmann^{a,b,c}, Martin A. B. Hedegaard^{a,b,c,e}, Thomas Von Erlach^{a,b,c}, Matthew O'Donnell^a, Frank R. Burden^f, David A. Winkler^{f,g,h}, and Molly M. Stevens^{a,b,c,1}

Departments of ^aMaterials and ^bBioengineering and ^cInstitute of Biomedical Engineering, Imperial College London, London SW7 2AZ, United Kingdom; ^dCraniofacial Development and Stem Cell Biology, King's College London, London SE1 9RT, United Kingdom; ^eDepartment of Chemical Engineering, Biotechnology and Environmental Technology, University of Southern Denmark, DK-5230 Odense, Denmark; ^fCell Biology Group, Biomedical Manufacturing Program, CSIRO Manufacturing Flagship, Clayton 3168, VIC, Australia; ^gMonash Institute of Pharmaceutical Sciences, Parkville 3052, VIC, Australia; and ^hLatrobe Institute of Molecular Science, Latrobe University, Bundoora 3086, VIC, Australia

Edited by Kristi S. Anseth, Howard Hughes Medical Institute, University of Colorado Boulder, Boulder, CO, and approved February 27, 2015 (received for review October 15, 2014)

Despite the increasing sophistication of biomaterials design and functional characterization studies, little is known regarding cells' global response to biomaterials. Here, we combined nontargeted holistic biological and physical science techniques to evaluate how simple strontium ion incorporation within the well-described biomaterial 4555 bioactive glass (BG) influences the global response of human mesenchymal stem cells. Our objective analyses of whole gene-expression profiles, confirmed by standard molecular biology techniques, revealed that strontium-substituted BG up-regulated the isoprenoid pathway, suggesting an influence on both sterol metabolite synthesis and protein prenylation processes. This up-regulation was accompanied by increases in cellular and membrane cholesterol and lipid raft contents as determined by Raman spectroscopy mapping and total internal reflection fluorescence microscopy analyses and by an increase in cellular content of phosphorylated myosin II light chain. Our unexpected findings of this strong metabolic pathway regulation as a response to biomaterial composition highlight the benefits of discovery-driven nonreductionist approaches to gain a deeper understanding of global cell-material interactions and suggest alternative research routes for evaluating biomaterials to improve their design.

strontium-releasing biomaterials | human mesenchymal stem cells | microarray analysis | sparse feature selection analysis | mevalonate pathway

An important aim of regenerative medicine is to design smart biomaterials to trigger specific biological responses and enable complex tissue repair (1). Standard in vitro and in vivo testing of such materials usually focuses on assessing the anticipated cell response, often stem cell differentiation to a particular lineage and/or appropriate tissue formation. Although this strategy allows the characterization of specific outcomes, the global cell responses to most biomaterials remain relatively unknown and their mechanisms of action largely unidentified. In comparison with this standard approach, the pharmacology and molecular biology communities have revolutionized their respective fields by taking advantage of unsupervised “-omic” technologies that allow the global biological response to be examined without the inherent bias introduced by predicting particular outcomes. The adoption of comparable hypothesis-generating holistic approaches in the biomaterials communities could stimulate a similar paradigm shift, allowing prospective, rational material design instead of retrospective material evaluation.

With more than 2.2 million bone-grafting procedures carried out annually worldwide, the market for smart biomaterials that can be used as functional alternatives to current autogenic and allogenic grafts is significant (2). One biomaterial-based regenerative approach involves the incorporation of biologically active moieties into biomaterials to enhance their bone regeneration properties (3). Strontium ranelate (SrRan) reduces vertebral and nonvertebral fractures in osteoporotic women (4, 5). Although the mechanism of action of SrRan is not fully understood (6, 7),

strontium ions have been reported to be the active component of the drug. Incorporating strontium into biomaterials has been shown to up-regulate osteogenic markers in vitro and osteoconduction in vivo (8–12); however, how such strontium-doped biomaterials improve clinical outcomes and, importantly, how such biomaterials influence the global response of osteoprogenitor cells are largely unknown.

To demonstrate this alternative approach of examining cell response to biomaterials, we applied whole-genome microarray techniques to the classic biomaterial bioactive glass (BG) after incorporation of strontium. Combining an atypical method for recognizing important features in data and Raman spectroscopy mapping, we examined the global response of bone marrow-derived human mesenchymal stem cells (hMSC). Surprisingly, our results show that, rather than directly up-regulating osteogenic genes, strontium-substituted BG (SrBG) strongly regulated the steroid biosynthesis pathway, suggesting a potential mode of action and an alternative avenue for further study. These data show the potential for nonreductionist discovery-driven approaches to transform the design of biomaterials and improve clinical outcomes, particularly in bone regeneration.

Results

Experimental Design. Upon exposure to biological fluids, BGs undergo localized dissolution/precipitation reactions, modifying their surrounding ionic environment. To mimic such environments,

Significance

Although new-generation biomaterials are increasingly complex and sophisticated, their development remains largely empirical, and functional outcomes are difficult to predict. Extending the biological evaluation of biomaterials beyond the assessment of presumed effects would allow a better understanding of the material-driven cell responses. Here we illustrate how applying an objective, nondiscriminative approach to explore the global cell responses to a series of bone substitutes with various compositions can uncover unexpected, important changes at the gene and cellular levels and can provide in-depth knowledge of the effects of specific material properties on cell behavior.

Author contributions: H.A., E.G., and M.M.S. designed research; H.A., E.G., E.L., M.A.B.H., and T.V.E. performed research; M.O. and D.A.W. contributed new reagents/analytic tools; H.A., E.G., E.L., M.A.B.H., T.V.E., F.R.B., and D.A.W. analyzed data; and H.A., E.G., D.A.W., and M.M.S. wrote the paper.

Conflict of interest statement: M.M.S. is a coinventor on intellectual property on strontium-containing bioactive glasses (WO2007/144662).

This article is a PNAS Direct Submission.

Freely available online through the PNAS open access option.

¹To whom correspondence should be addressed. Email: m.stevens@imperial.ac.uk.

This article contains supporting information online at www.pnas.org/lookup/suppl/doi:10.1073/pnas.1419799112/-DCSupplemental.

BGs based on the 45S5 composition in which 0, 10, and 100 mol% of calcium was replaced by strontium (Sr0, Sr10, and Sr100, respectively) were incubated with hMSC growth culture medium and subsequently filtered to remove BG particles (Fig. S1A), creating BG-conditioned medium. Inductively coupled plasma optical emission spectroscopy (ICP-OES) demonstrated that, although the silicon and phosphate concentrations were similar in all BG-conditioned medium compositions, strontium concentrations increased with increasing strontium substitution (Fig. S1B).

hMSC from three donors were exposed to SrBG-conditioned medium for 30 min, 2 h, 4 h, 48 h, 5 d, or 10 d, with medium refreshed with new conditioned medium over the course of the experiment. Whole-genome microarray analyses were carried out, and data were examined using an atypical approach to feature selection and an objective functional annotation clustering analysis. Further investigations of cell response were performed using quantitative real-time PCR, Western blotting and in-cell Western blotting, Raman spectroscopy mapping, and total internal reflection fluorescence (TIRF) microscopy.

Regulation of hMSC Gene Expression by BG and SrBG Dissolution Products. Initial statistical analysis indicated that all BG-conditioned media triggered significant modifications of hMSC mRNA expression in more than 1,000 genes compared with control (CTL) growth medium (Fig. 1A). With respect to BG composition, the total number of genes and particularly the number of highly significant differentially expressed (DE) genes increased with increasing strontium substitution, suggesting a more profound modification of the hMSC expression profile with exposure to SrBG dissolution products.

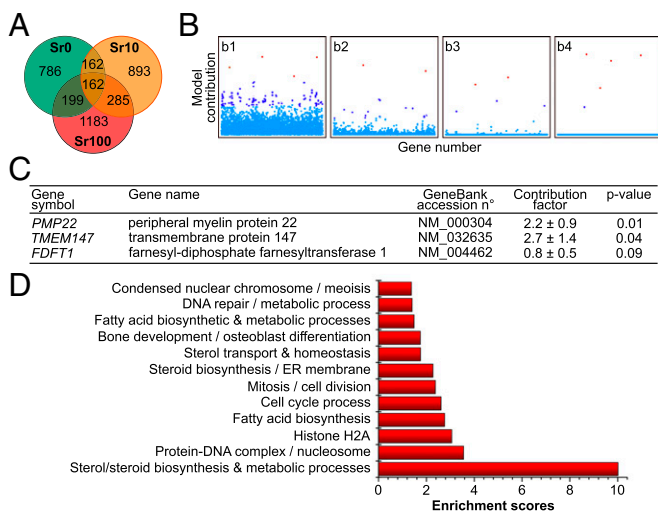


Fig. 1. Changes in hMSC global mRNA expression mediated by treatment with BG- and SrBG-conditioned media. (A) Venn diagram depicting the number of genes differentially expressed (with $P < 0.05$) in response to BG and SrBG exposure, compared with the CTL group. (B) Illustration of the operation of the EM algorithm, showing progressive setting to zero for the genes least relevant to the SrBG treatment to identify a small set of key genes (B, 1–B, 4). (C) Table of the most significant discriminators identified by sparse feature analysis of the hMSC response to treatment with SrBG-conditioned medium. The contribution, expressed as mean \pm SE, is an indication of that gene's importance in the model discriminating the effect of the treatment conditions. Positive values indicate up-regulation in response to SrBG exposure. P values represent the Student's t test confidence level for each gene's contribution to the model. (D) Graphic representation of the functional annotation clustering analysis of the genes differentially expressed in response to Sr100 treatment compared with CTL treatment, highlighting a strong enrichment score of the sterol-steroid biosynthesis and metabolic processes.

To identify key genes involved in the hMSC response, we analyzed the dataset using an expectation maximization (EM) algorithm. This method of sparse feature selection is an unbiased approach that is very useful for identifying small sets of relevant genes in large microarray datasets in a context-dependent manner by progressively setting the contributions of less relevant genes to zero (Fig. 1B) (13). We added two extra hyperparameters, χ and ζ , so that the sparsity of the selection method could be varied (14, 15).

The EM algorithm method selected a limited set of 11 genes whose expression patterns were altered significantly in the presence of SrBG-conditioned medium. In particular, three of the genes selected by this very sparse selection method acted as clear discriminators between cultures with and without SrBG treatment across the ranges of Sr^{2+} concentrations in the experiment (Fig. 1C). These genes were transmembrane protein 147 (TMEM147), peripheral myelin protein 22 (PMP22), and farnesyl-diphosphate farnesyltransferase 1 (squalene synthase, FDFT1). TMEM147 is a transmembrane protein found exclusively in the endoplasmic reticulum that binds to cholesterol (16) and G protein-coupled receptors (GPCR) (17). PMP22 (also known as "GAS3") is a glycoprotein associated with lipid rafts that modulates apoptosis, cell morphology, actin stress formation, and migration (19, 20). FDFT1 is a key mediator of the isoprenoid biosynthesis pathway where it catalyzes the first reaction of the branch committed to sterol biosynthesis. As such, the regulation of FDFT1 directs the formation of either sterol or nonsterol metabolites (21). Although differences in cell metabolic profiles during hMSC commitment and differentiation have been reported previously (22, 23), this result represented an unexpected finding because both BG and strontium had been presumed primarily to up-regulate bone formation and/or differentiation of osteoprogenitor cells (7, 24).

To understand better the global expression modifications in hMSC in response to BG/SrBG treatment, we next applied a functional annotation clustering analysis to the DE genes. When comparing SrBG and CTL conditions, we identified a strong regulation of a cluster of genes in the sterol and steroid biosynthesis pathways (Fig. 1D and Table S1). This cluster showed high enrichment (enrichment score >10) and significance ($P < 10^{-13}$) and was accompanied by several correlated clusters implicated in sterol and steroid biosynthesis, transport, and homeostasis or fatty acid biosynthetic and metabolic processes. These features were conserved among the Sr100 vs. CTL, Sr10 vs. CTL, and Sr100 vs. Sr0 groups. Such clusters were not identified in the Sr0 vs. CTL condition, suggesting that strontium incorporation played a role in this regulation. Taken together, these results suggest that strontium in BG has a profound effect on the regulation of the sterol/sterol biosynthesis and the associated metabolic processes, supporting our initial finding of the critical role of FDFT1 in response to SrBG.

As has been hypothesized, we also identified the regulation of genes associated with bone development, osteoblast differentiation, and bone mineralization with SrBG treatment (Fig. 1D and Table S1). However, the enrichment scores of these clusters (1.42–1.98) were lower than those described above, and the expression patterns were similar for all BG treatments with no differences identified among BG compositions. For example, hMSC exposed to SrBG medium for 5 d induced up-regulation of secreted phosphoprotein 1 (also known as osteopontin), glycoprotein (transmembrane) nmb, and BMP2 (bone morphogenetic protein 2) compared with CTL ($P < 0.05$, Sr10 vs. CTL) (Fig. S2). Taken together, these observations suggest that, although genes associated with osteoblast differentiation were indeed differentially regulated in response to BG and SrBG, the effects were subtle and were not strongly affected by strontium. Instead, the primary regulators of hMSC response were genes involved in the sterol and steroid biosynthesis and metabolic processes.

Up-Regulation of the Mevalonate and Steroid Biosynthesis Pathways in SrBG-Treated hMSC. Considering that SrBG strongly regulated sterol and steroid biosynthesis and metabolic process clusters, we next asked whether the amount of strontium in BG was also a factor. Kyoto Encyclopedia of Genes and Genomes (KEGG) pathway analyses highlighted that, compared with CTL, Sr100 and Sr10 significantly regulated 11 and 13, respectively, of the 13 genes encoding enzymes of the mevalonate pathway and its downstream steroid biosynthesis pathway (Fig. S34). These pathways mediate cellular processes including sterol-steroid synthesis, protein prenylation, cell membrane maintenance, and N-glycosylation (25). Further analyses confirmed similar expression profiles of the enzyme-coding genes from these two pathways (Fig. 2A and Fig. S3B), with significant increases in mRNA expression over time up to day 5 correlating with increasing strontium content in BG.

To confirm these observations, we performed RT-PCR on representative genes from these pathways after 5 d of exposure to BG or SrBG (Fig. 2B). The expression of *HMGCS1* [3-hydroxy-3-methylglutaryl-CoA synthase 1 (soluble)], *HMGCR* (3-hydroxy-3-methylglutaryl-CoA reductase), *FDPS* (farnesyl diphosphate synthase), and *SC4MOL* (also known as *MSMO1*, methylsterol monooxygenase 1) was increased significantly compared with $t = 0$ and was significantly higher in all cells treated with SrBG-conditioned medium than in cells treated with CTL medium. Interestingly, hMSC exposure to Sr0 similarly triggered a significant increase in *HMGCS1*, *HMGCR*, and *SC4MOL* expression. However, Sr100 significantly up-regulated *HMGCS1* and *HMGCR* compared with Sr0, and *SC4MOL* was significantly up-regulated in

Sr100-treated hMSC compared with Sr0 and Sr10 treatment. These experiments corroborated the findings from the microarray dataset, confirming the significant influence of strontium incorporated within BG biomaterials on hMSC gene regulation.

Because gene expression does not necessarily correlate with protein translation, we then sought to evaluate the influence of the regulation of mRNA expression at the protein level with in-cell Western blots (Fig. 2C). Although no significant modification of the amount of *HMGCS1* was detected among the various conditions, SrBG treatment significantly increased the cellular content of *FDFT1* and geranylgeranyl diphosphate synthase 1 (*GGPS1*), two key enzymes at the branching point of the isoprenoid pathway (21, 26, 27). *GGPS1*, together with *FDPS*, mediates the protein prenylation process essential for membrane attachment of proteins, whereas *FDFT1* controls the synthesis of sterol metabolites, which, after enzymatic modifications, results in the formation of cholesterol. Although the amount of *FDFT1* and *GGPS1* tended to increase in the Sr10 and Sr100 groups, respectively, compared with the Sr0 group, no significant differences were found between the BG conditions. In accordance with our gene-expression analyses, these differences in protein expression suggested that SrBG-conditioned media influenced both the sterol- and nonsterol-committed branches of the isoprenoid pathway.

Enrichment of Cell Cholesterol and Lipid Content After Exposure of hMSC to SrBG-Conditioned Medium. Given our observations of dramatic modifications in mRNA and protein expression of enzymes from the mevalonate and steroid biosynthesis pathways, we hypothesized that SrBG treatment also would affect cell sterol metabolite content. Raman spectroscopy is capable of providing detailed biochemical characterization of live cell cultures and is similar to the microarray analyses in that it is a nondiscriminate, unbiased technique (28–30). Therefore, we applied Raman spectroscopy mapping to hMSC treated with SrBG-conditioned medium (Fig. 3). The characteristic spectra that were identified by *k*-means clustering analysis and represent distinctive cell signatures were classified as medium and high cholesterol/lipid content, nucleus, or cytoplasm (Fig. 3A and Fig. S4). This Raman spectrum clustering analysis highlighted clear discrimination between the experimental conditions. The strongest discriminator proved to be cell lipid and cholesterol content, an important end product of the sterol biosynthesis pathway. As shown in Fig. 3B and C, a significantly higher percentage of lipid/cholesterol-rich spectra per cell was observed in hMSC after exposure to Sr100 than after exposure to CTL medium. These results are in line with our previous findings and indicate that the up-regulation of the sterol biosynthesis pathway triggered an increase in cell sterol metabolites.

hMSC Enrichment of Membranous Cholesterol and Lipid Rafts in Response to SrBG-Conditioned Medium. Cholesterol is a crucial component of the lipid bilayer of mammalian cell membranes and is a key player in the regulation of physical properties such as rigidity and permeability and of membrane protein clustering and activity (31). Our observations of up-regulation of *FDFT1*, which is known to be related to membrane lipid raft content (26), and increased cell cholesterol content as determined Raman spectroscopy led us to speculate that SrBG biomaterials affected the cellular production of the cholesterol- and sphingolipid-enriched membrane microdomains known as “lipid rafts.” Such raft-signaling platforms have been shown to be important for numerous signaling pathways and cell functions. For example, they regulate the activity of various GPCRs and ion channels as well as integrin- and small GTPase-mediated signaling events (32–35).

To explore this possibility, we used TIRF microscopy to visualize and quantify cholesterol content and lipid rafts at or near hMSC plasma membranes in response to SrBG treatment. We observed significantly higher signal intensity of filipin III on the substrate-facing plasma membrane in hMSC treated with Sr100-conditioned

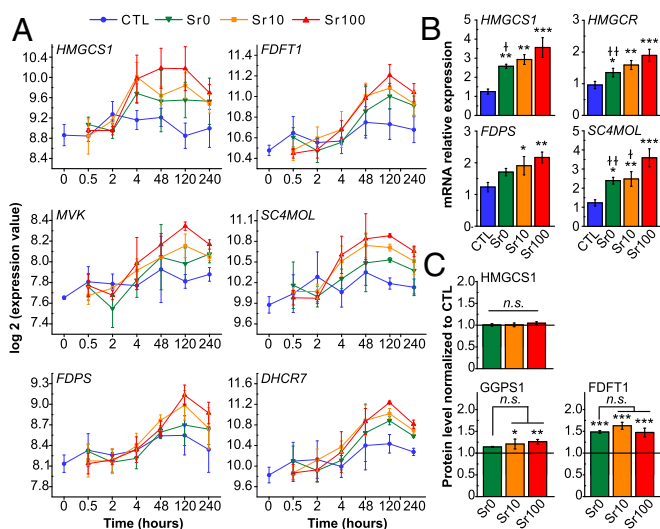


Fig. 2. Regulation of mRNA and protein expression of enzyme-coding genes from the mevalonate and steroid biosynthesis pathways by SrBG-conditioned media. (A) Expression profiles of selected genes representative of various stages of the mevalonate and sterol-steroid biosynthesis pathways, showing an increase of mRNA expression levels over time and with increasing amounts of strontium within the BG. Data were extracted from the microarray dataset. (B) *HMGCS1*, *HMGCR*, *FDPS*, and *SC4MOL* mRNA expression, relative to $t = 0$, in hMSC after 5 d of culture in the presence of CTL or BG-conditioned media quantified by real-time PCR validating the results obtained by the microarray analysis. The 5-d exposure period was chosen based on microarray analyses, because hMSC displayed the strongest differential gene expression in response to the treatments at this time point. (C) Protein levels of *HMGCS1*, *FDFT1*, and *GGPS1* normalized to DNA content and relative to the CTL group (dashed line) after 5 d of treatment measured by in-cell Western blotting. All data are expressed as mean \pm SD, $n = 3$. In B and C, asterisks and daggers represent significant differences of the marked bars compared with the CTL group and compared with Sr100 treatment, respectively (* $P < 0.05$; ** $P < 0.01$; *** $P < 0.001$; $^{\dagger}P < 0.05$; $^{\dagger\dagger}P < 0.01$). n.s., no significant differences between the SrBG groups and Sr0.

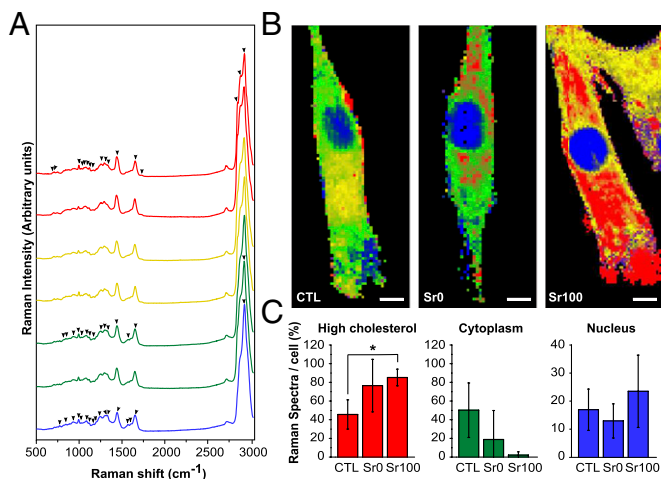


Fig. 3. Raman spectroscopy mapping evidence of increased cholesterol and lipid content in hMSC treated with Sr100 medium. Raman spectroscopy mapping was performed on hMSC treated for 5 d with CTL, Sr0, or Sr100 medium. (A) Characteristic spectra identified by *k*-means cluster analysis of cell-distinctive signatures. Characteristic spectra were classified as nucleus (blue), cytoplasm (green), medium lipid/cholesterol content (yellow), and high lipid/cholesterol content (red). Arrowheads mark characteristic differences among spectra (see Fig. S4 for details). (B) Artificially colored representative images of characteristic spectra within cells. Colors correspond to the spectra assignment in A. (Scale bars, 10 μ m.) (C) Quantification of the percentage of spectra per cell that are characteristic of lipid/cholesterol-rich regions (medium and high amounts), cytoplasm, or the nucleus. Data are expressed as mean \pm SD, $n = 4$. * $P < 0.05$.

medium than in hMSC treated with either Sr0 or CTL medium (Fig. 4 A and B). Filipin III binds nonesterified sterols and is used for the identification of cellular cholesterol (36). To investigate further an effect of SrBG treatment on lipid raft formation, we used FITC-conjugated cholera toxin B subunit (CTB), which has been reported to bind specifically to lipid rafts and is commonly used for their identification (37). CTB analyses by TIRF revealed significantly higher staining intensity in hMSC exposed to Sr100 than in hMSC exposed to CTL (Fig. 4 C and D). Taken together, these experiments indicate that the formation of plasma membrane lipid rafts is affected by exposure to SrBG-conditioned medium. Given the broad cell-signaling implications of lipid rafts (35), this observation opens the intriguing possibility that these particular cell-biomaterial responses may be mediated by changes in the cell plasma membrane.

Increase in the Amount of Phosphorylated Myosin II Light Chain in SrBG-Treated hMSC. Lipid raft-regulated signaling cascades are modulated through interactions with the actin/myosin meshwork (32, 38). The communication between the cytoskeleton and lipid rafts is ensured by the presence of several membrane skeleton proteins such as actin, tubulin, or myosin II (38, 39) within these cholesterol-rich domains and is modulated by small GTPases that are targeted to the membrane as a result of FDPS/GGPI1-mediated prenylation. The increase in lipid rafts and *FDPS* and *GGPI1* expression observed in response to SrBG led us to investigate whether SrBG-conditioned media may modulate hMSC actin/myosin activity further. We quantified the cellular content of the active phosphorylated form of myosin II light chain (pMLC) by Western blotting after hMSC exposure to BG or SrBG for 5 d (Fig. 4 E and F). Densitometry analyses of pMLC revealed a systematic increase in pMLC content in the Sr10 and Sr100 conditions as compared with the CTL and Sr0 conditions. This result suggested that strontium incorporated within the BG had an effect on the actin/myosin meshwork, which is already known to be an important regulator of hMSC commitment (40, 41).

Discussion

Here, we exploited the potency of unbiased, nontargeted approaches to investigate how changes in the local cellular environment triggered by strontium substitution in BG influences global hMSC response. Cell-culture models based on conditioned media have been used widely in previous studies (8, 24, 42, 43), because the local ion content near the material's surface upon implantation is likely to affect the cellular response, along with its surface properties (44). The strontium concentration in SrBG-conditioned media was dependent on the level of Sr substitution in BG (0 mM, 0.1 mM, and 1 mM for Sr0, Sr10, and Sr100, respectively). Such concentrations are likely to be clinically relevant, because the median strontium serum concentration in patients treated with SrRan is 0.12 mM (4), and 1 mM has been used as a reference concentration in several in vitro studies (45, 46).

Our whole-genome microarray analyses revealed the influence of SrBG on hMSC gene expression, with more profound effects observed in groups treated with higher levels of strontium in the biomaterial. Subsequent analyses of the array data demonstrated an increased expression of genes encoding enzymes from the mevalonate and sterol biosynthesis pathways, suggesting strong up-regulation of the sterol and steroid biosynthesis and metabolic processes and protein prenylation activity. These differences were translated to the protein and cellular levels as determined by in-cell Western blot and cholesterol content measurements by Raman spectroscopy. We observed that, as did Sr10 and Sr100, Sr0 exerted a mild effect on many processes, suggesting an influence of the BG-modified ionic environment itself. However, a correlation between the amount of strontium incorporated

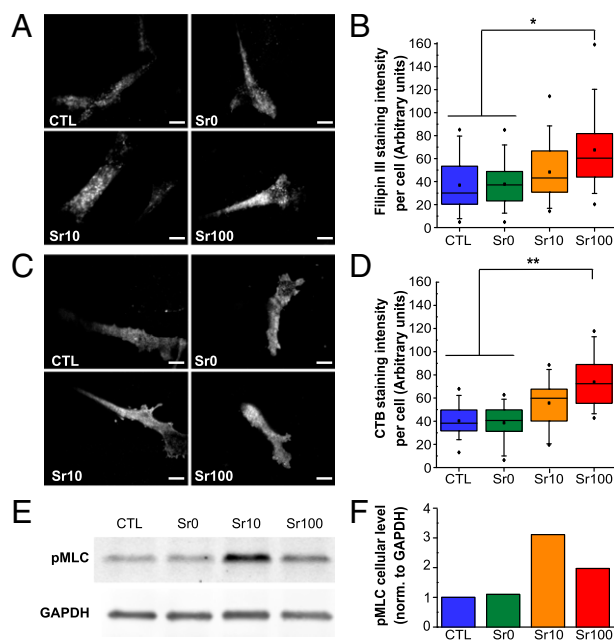


Fig. 4. Increased cholesterol and lipid raft content at the cell membrane and cellular content of pMLC in response to SrBG treatment. (A and B) Representative TIRF images (A) and quantification of filipin III abundance (B) as a marker of nonesterified cholesterol content at the cell membrane of hMSC treated for 5 d with CTL, BG-, or SrBG-conditioned media. (C and D) Representative TIRF images (C) and quantification of CTB abundance (D) as a marker of lipid raft content at the cell membrane of hMSC treated for 5 d with CTL, BG-, or SrBG-conditioned media. (Scale bars, 10 μ m.) In B and D data are presented as box plots and represent analysis of more than 30 cells per group. * $P < 0.05$, $n = 3$. (E and F) Representative Western blot (E) and densitometry quantification (F) of pMLC cellular content (relative to GAPDH) in hMSC after 5 d of treatment with BG- or SrBG-conditioned media. E and F are representative of three independent experiments.

within BG and the up-regulation of these pathways was supported by significant differences between the Sr100 and Sr0 treatments. Interestingly, Sr100 exposure led to changes in the membrane composition of hMSC as characterized by increases in membrane cholesterol and lipid raft contents, and treatment of hMSC with Sr10 and Sr100 further led to an increase of the amount of cellular pMLC. Such effects on plasma membrane composition and myosin activity were not found in hMSC treated with Sr0, strengthening the hypothesis that the strontium incorporated within BG mediates these important physiological changes.

Previous studies assessing the effects of bone-regenerative biomaterials on gene expression using ChIP arrays often focused on specific genes or clusters known to play roles in osteogenesis but were silent on other biological responses. Others have aimed to identify potential key regulators of cell response to biomaterials and have provided lists of DE genes (43, 47–49). Although these studies highlight important possibilities, it remains challenging to interpret the importance of individual DE genes outside their biological context or draw conclusions regarding their physiological importance. Here we chose to combine the objectivity of a functional annotation clustering analysis with a sparse feature selection approach that allowed the detection of a small number of biologically significant genes in a context-dependent manner. More than 1,000 genes were significantly regulated in hMSC after treatment with SrBG-conditioned medium, making the task of manually identifying key genes extremely challenging. In contrast, the sparse feature selection method produced models that made biological interpretation simpler because fewer explanatory variables were required; this method previously has been shown to outperform the commonly used support vector machine algorithm (13). The sparse feature selection method unexpectedly identified genes encoding PMP22, TMEM147, and FDFT1. The up-regulation of the lipid raft-interacting protein PMP22 (18) and the transmembrane protein TMEM147, which is known to bind to cholesterol (16), appeared coherent with the changes in mRNA expression of FDFT1, which controls the synthesis of sterol metabolites (21) and regulates the lipid raft content of the cell membrane (26). This finding led us to propose a new hypothesis regarding SrBG regulation of hMSC based on these pathways, membrane cholesterol content, and lipid rafts.

PMP22 was previously highlighted in a microarray-based study as one of the few genes in human osteoblasts up-regulated by treatment with 45S5 BG-conditioned medium (43), suggesting that PMP22 plays an important role in both osteoblast and hMSC response. However, further analyses were not pursued in previous studies, perhaps because PMP22 failed to fit standard hypotheses regarding cell response to biomaterials and particularly BG. Conversely, our sparse selection analysis led us to investigate the regulation of these genes, directly leading to our discovery of the regulation of the sterol synthesis pathway and subsequent modification of membrane cholesterol and lipid rafts in hMSC response to SrBG. This finding is exciting because lipid rafts are dynamic microdomains of the plasma membrane that play key roles in regulating most of the signaling pathways at the cell surface, including EGF receptor, Hedgehog, Ras, and integrin transduction signaling processes (35), that subsequently lead to the modulation of numerous cell functions (32). These functions are regulated by the combined influence of cholesterol binding with membrane proteins, such as GPCR, ion channels, or integrins, and the control of their segregation/clustering within raft-signaling platforms through actin/myosin cytoskeleton meshwork (32). Communication between raft-signaling platforms and the actin/myosin cytoskeleton is essential for the modulation of signaling cascades, and this interaction is mediated by small GTPases (32). The membrane targeting and subsequent activity of small GTPase proteins requires an initial prenylation step ensured by FDPS and GGPS1. Here, we observed that SrBG treatment not only increased lipid raft content but also up-regulated *FDPS* and *GGPS1*

mRNA expression and GGPS1 protein expression. This up-regulation indicated a possible modulation of small GTPase-mediated cell functions, such as cell proliferation, migration, spreading, or cytoskeleton arrangement (33, 50). For example, phosphorylation of myosin II light chain, which is essential in actin/myosin meshwork activity and cell contractility, is regulated by the rho-family small GTPases (51) and previously has been reported to be reduced after the inhibition of the mevalonate pathway (52). Moreover, our observation of the increase of active pMLC in the presence of SrBG appeared consistent with the up-regulation of the isoprenoid biosynthesis pathway and demonstrated that strontium incorporation within the BG had an effect on actomyosin activity. This last result is particularly interesting because cytoskeletal arrangement, which is modulated by environmental calcium and strontium (46, 47), is known to influence hMSC lineage commitment, particularly during osteogenesis (53), as a result of the modulation of actin/myosin cytoskeletal contraction (40, 41, 49), and was found to modulate cell metabolic profiles (22). Together, our data suggest that the up-regulation of the mevalonate and sterol biosynthesis pathways in hMSC and subsequent membrane cholesterol and lipid raft enrichment in response to SrBG likely change membrane protein quantity or activity. Along with the increase of myosin II light chain activity in SrBG-treated hMSC, these effects open the possibility of further cell-signaling modulations.

Analysis of our array data also highlighted effects, although notably less pronounced, of SrBG treatment on the expression of genes involved in osteoblast differentiation, bone development, and mineralization. Although only a few osteoblastic genes were differentially expressed, the expression profiles were consistent with those previously reported in response to modified ionic environments (42, 47). *BMP2*, which encodes bone morphogenetic protein-2, was one of the few genes up-regulated by SrBG and is an osteoinductive growth factor whose expression has been shown to increase in response to calcium and strontium (12, 47). Such gene regulations may suggest a progressive commitment of hMSC toward the osteoblastic lineage in response to SrBG exposure. Under the conditions tested here, we did not identify statistical differences between BG compositions in the regulation of osteoblast-related genes. However, such results may not be surprising, because the *in vitro* effects of soluble strontium (or SrRan) on osteoblastic activity and gene expression have been shown to be subtle (46) and difficult to discern from the effects of calcium, given that both ions affect several similar pathways (7).

In a field in which biomaterials design is increasingly complex, it is interesting to note that the simple inclusion of an ion, such as strontium, within a well-characterized material structure can induce important changes in gene expression, metabolic pathways, and the membrane composition of osteoprogenitor cells. However, because the mechanisms of action of material-driven bone regeneration remain to be elucidated, the development of new biomaterials may prove more efficient with methods that better probe the true response of cells to materials. As we show here, the use of objective screening methods can allow the characterization of global cell responses and are not restricted by a priori assumptions. With the development of increasingly complex and active biomaterials, applying such discovery-driven approaches to study biological responses from various classes of materials may be beneficial for the rational design of materials for regenerative medicine applications. The resulting development of *in vitro* models that effectively predict the efficacy of biomaterials then may streamline the translation of the biomaterials with the highest potential from the bench to the clinic.

Experimental Procedures

Cell Culture. Bone marrow-derived hMSC from three donors were obtained commercially, expanded, and used independently for microarray experiments and subsequent analyses.

BG- and SrBG-Conditioned Medium. BG particles (0, 10, or 100 mol% substitution of calcium with strontium) were incubated in cell culture medium for 24 h at 37 °C and then removed.

Microarray Study. hMSC were treated with basal, BG, or SrBG media for 30 min, 2 h, 4 h, 24 h, 48 h, 5 d, or 10 d. After RNA extraction and sample preparation, whole genome expression analyses were performed using Affymetrix HuGene arrays. Data were examined using a sparse feature selection method, functional clustering, and KEGG analyses.

Molecular Biology and Biochemistry. After 5 d, RT-PCR, Western, and in-cell Western blotting were carried out using standard methods to verify expression of genes in the isoprenoid pathway (identified by microarray) and their translation.

TIRF Microscopy. Fixed hMSC were incubated with FITC-CTB or Fillipin III and imaged on a Zeiss Axiovert 200.

Raman Spectroscopy. Fixed hMSC were mapped on a Renishaw RM 2000. Data were analyzed in MatLab using a *k*-means cluster analysis.

Statistical Analyses. A one-way ANOVA with a post hoc Tukey test was used to determine significance unless indicated otherwise. Details of the experimental procedures are available in *SI Experimental Procedures*.

ACKNOWLEDGMENTS. We thank Ms. S. Skeete for laboratory assistance; Dr. S. Sampson and Prof. T. Cass for providing equipment access and training; Dr. L. Game and Ms. N. Lambie, from the Genomics Laboratory of the Clinical Science Center, Imperial College London, for advice regarding the design of the microarray experiment and for the ChIP hybridization and scanning, respectively; and Dr. G. R. Barton from the Bioinformatics Support Service, Imperial College London, for statistical analysis and assistance in the analysis of the microarray dataset and the study design. M.M.S. and H.A. were supported by the Medical Engineering Solutions in Osteoarthritis Centre of Excellence funded by the Wellcome Trust and the Engineering and Physical Sciences Research Council. M.M.S. was also supported by the Technology Strategy Board, United Kingdom, and the Rosetrees Trust. H.A. was partially supported by the VIP award from the Wellcome Trust. E.L. was supported by European Commission funding under the 7th Framework Programme Marie Curie Initial Training Networks Grant 289958, bioceramics for bone repair. E.G. is supported by a Research Career Development Fellowship from the Wellcome Trust. M.A.B.H. was partially supported by The Danish Council for Independent Research (Technology and Production Sciences contract 0602-02350B). D.A.W. is the recipient of a Newton Turner Fellowship for Exceptional Senior Scientists.

- Place ES, Evans ND, Stevens MM (2009) Complexity in biomaterials for tissue engineering. *Nat Mater* 8(6):457–470.
- Pashuck ET, Stevens MM (2012) Designing regenerative biomaterial therapies for the clinic. *Sci Transl Med* 4(160):160sr4.
- Bose S, Fielding G, Tarafder S, Bandyopadhyay A (2013) Understanding of dopant-induced osteogenesis and angiogenesis in calcium phosphate ceramics. *Trends Biotechnol* 31(10):594–605.
- Meunier PJ, et al. (2004) The effects of strontium ranelate on the risk of vertebral fracture in women with postmenopausal osteoporosis. *N Engl J Med* 350(5):459–468.
- Reginster JY, et al. (2005) Strontium ranelate reduces the risk of nonvertebral fractures in postmenopausal women with osteoporosis: Treatment of Peripheral Osteoporosis (TROPOS) study. *J Clin Endocrinol Metab* 90(5):2816–2822.
- Stepan JJ (2013) Strontium ranelate: In search for the mechanism of action. *J Bone Miner Metab* 31(6):606–612.
- Saidak Z, Marie PJ (2012) Strontium signaling: Molecular mechanisms and therapeutic implications in osteoporosis. *Pharmacol Ther* 136(2):216–226.
- Gentleman E, et al. (2010) The effects of strontium-substituted bioactive glasses on osteoblasts and osteoclasts in vitro. *Biomaterials* 31(14):3949–3956.
- Newman SD, et al. (2014) Enhanced osseous implant fixation with strontium-substituted bioactive glass coating. *Tissue Eng Part A* 20(13–14):1850–1857.
- O'Donnell MD, Candarlioglu PL, Miller CA, Gentleman E, Stevens MM (2010) Materials characterisation and cytotoxic assessment of strontium-substituted bioactive glasses for bone regeneration. *J Mater Chem* 20(40):8934–8941.
- Park J-W, et al. (2010) Osteoblast response and osseointegration of a Ti-6Al-4V alloy implant incorporating strontium. *Acta Biomater* 6(7):2843–2851.
- Zhang W, et al. (2013) The synergistic effect of hierarchical micro/nano-topography and bioactive ions for enhanced osseointegration. *Biomaterials* 34(13):3184–3195.
- Figueiredo MAT (2003) Adaptive sparseness for supervised learning. *IEEE Trans Pattern Anal Mach Intell* 25(9):1150–1159.
- Burden FR, Winkler DA (2009) Optimal sparse descriptor selection for QSAR using Bayesian methods. *QSAR Comb Sci* 28(6–7):645–653.
- Burden FR, Winkler DA (2009) An optimal self-pruning neural network and nonlinear descriptor selection in QSAR. *QSAR Comb Sci* 28(10):1092–1097.
- Hulce JJ, Cognetta AB, Niphakis MJ, Tully SE, Cravatt BF (2013) Proteome-wide mapping of cholesterol-interacting proteins in mammalian cells. *Nat Methods* 10(3):259–264.
- Rosemond E, et al. (2011) Regulation of M₃ muscarinic receptor expression and function by transmembrane protein 147. *Mol Pharmacol* 79(2):251–261.
- Hasse B, Bosse F, Müller HW (2002) Proteins of peripheral myelin are associated with glycosphingolipid/cholesterol-enriched membranes. *J Neurosci Res* 69(2):227–232.
- Brancolini C, et al. (1999) Rho-dependent regulation of cell spreading by the tetraspan membrane protein Gas3/PMP22. *Mol Biol Cell* 10(7):2441–2459.
- Zoltewicz SJ, et al. (2012) The palmitoylation state of PMP22 modulates epithelial cell morphology and migration. *ASN Neuro* 4(6):409–421.
- Do R, Kiss RS, Gaudet D, Engert JC (2009) Squalene synthase: A critical enzyme in the cholesterol biosynthesis pathway. *Clin Genet* 75(1):19–29.
- Tsimbouri PM, et al. (2012) Using nanotopography and metabolomics to identify biochemical effectors of multipotency. *ACS Nano* 6(11):10239–10249.
- Reyes JMG, et al. (2006) Metabolic changes in mesenchymal stem cells in osteogenic medium measured by autofluorescence spectroscopy. *Stem Cells* 24(5):1213–1217.
- Hoppe A, Güldal NS, Boccaccini AR (2011) A review of the biological response to ionic dissolution products from bioactive glasses and glass-ceramics. *Biomaterials* 32(11):2757–2774.
- Goldstein JL, Brown MS (1990) Regulation of the mevalonate pathway. *Nature* 343(6257):425–430.
- Brusselmans K, et al. (2007) Squalene synthase, a determinant of Raft-associated cholesterol and modulator of cancer cell proliferation. *J Biol Chem* 282(26):18777–18785.
- McTaggart SJ (2006) Isoprenylated proteins. *Cell Mol Life Sci* 63(3):255–267.
- Gentleman E, et al. (2009) Comparative materials differences revealed in engineered bone as a function of cell-specific differentiation. *Nat Mater* 8(9):763–770.
- Swain RJ, Stevens MM (2007) Raman microspectroscopy for non-invasive biochemical analysis of single cells. *Biochem Soc Trans* 35(Pt 3):544–549.
- Swain RJ, Jell G, Stevens MM (2008) Non-invasive analysis of cell cycle dynamics in single living cells with Raman micro-spectroscopy. *J Cell Biochem* 104(4):1427–1438.
- Simons K, Ikonen E (2000) How cells handle cholesterol. *Science* 290(5497):1721–1726.
- Head BP, Patel HH, Insel PA (2014) Interaction of membrane/lipid rafts with the cytoskeleton: Impact on signaling and function: Membrane/lipid rafts, mediators of cytoskeletal arrangement and cell signaling. *Biochim Biophys Acta* 1838(2):532–545.
- Navarro-Lérica I, et al. (2012) A palmitoylation switch mechanism regulates Rac1 function and membrane organization. *EMBO J* 31(3):534–551.
- del Pozo MA, et al. (2004) Integrins regulate Rac targeting by internalization of membrane domains. *Science* 303(5659):839–842.
- Simons K, Toomre D (2000) Lipid rafts and signal transduction. *Nat Rev Mol Cell Biol* 1(1):31–39.
- Wüstner D (2007) Fluorescent sterols as tools in membrane biophysics and cell biology. *Chem Phys Lipids* 146(1):1–25.
- Blank N, et al. (2007) Cholera toxin binds to lipid rafts but has a limited specificity for ganglioside GM1. *Immunol Cell Biol* 85(5):378–382.
- Chichili GR, Rodgers W (2009) Cytoskeleton-membrane interactions in membrane raft structure. *Cell Mol Life Sci* 66(14):2319–2328.
- Nebi T, et al. (2002) Proteomic analysis of a detergent-resistant membrane skeleton from neutrophil plasma membranes. *J Biol Chem* 277(45):43399–43409.
- McBeath R, Pirone DM, Nelson CM, Bhadriraju K, Chen CS (2004) Cell shape, cytoskeletal tension, and RhoA regulate stem cell lineage commitment. *Dev Cell* 6(4):483–495.
- Engler AJ, Sen S, Sweeney HL, Discher DE (2006) Matrix elasticity directs stem cell lineage specification. *Cell* 126(4):677–689.
- Tsigkou O, Jones JR, Polak JM, Stevens MM (2009) Differentiation of fetal osteoblasts and formation of mineralized bone nodules by 45S5 Bioglass conditioned medium in the absence of osteogenic supplements. *Biomaterials* 30(21):3542–3550.
- Xynos ID, Edgar AJ, Buttery LDK, Hench LL, Polak JM (2001) Gene-expression profiling of human osteoblasts following treatment with the ionic products of Bioglass 45S5 dissolution. *J Biomed Mater Res* 55(2):151–157.
- Gentleman MM, Gentleman E (2014) The role of surface free energy in osteoblast-biomaterial interactions. *Int Mater Rev* 59(8):417–429.
- Fromiguet O, Haÿ E, Barbara A, Marie PJ (2010) Essential role of nuclear factor of activated T cells (NFAT)-mediated Wnt signaling in osteoblast differentiation induced by strontium ranelate. *J Biol Chem* 285(33):25251–25258.
- Bonnely E, Chabadel A, Saltel F, Jurdic P (2008) Dual effect of strontium ranelate: Stimulation of osteoblast differentiation and inhibition of osteoclast formation and resorption in vitro. *Bone* 42(1):129–138.
- Barradas AMC, et al. (2012) A calcium-induced signaling cascade leading to osteogenic differentiation of human bone marrow-derived mesenchymal stromal cells. *Biomaterials* 33(11):3205–3215.
- Barradas AMC, et al. (2013) Molecular mechanisms of biomaterial-driven osteogenic differentiation in human mesenchymal stromal cells. *Integr Biol (Camb)* 5(7):920–931.
- Kilian KA, Bugarija B, Lahn BT, Rksich M (2010) Geometric cues for directing the differentiation of mesenchymal stem cells. *Proc Natl Acad Sci USA* 107(11):4872–4877.
- Murali A, Rajalingam K (2014) Small Rho GTPases in the control of cell shape and motility. *Cell Mol Life Sci* 71(9):1703–1721.
- Amano M, et al. (1996) Phosphorylation and activation of myosin by Rho-associated kinase (Rho-kinase). *J Biol Chem* 271(34):20246–20249.
- Zeng L, et al. (2005) HMG CoA reductase inhibition modulates VEGF-induced endothelial cell hyperpermeability by preventing RhoA activation and myosin regulatory light chain phosphorylation. *FASEB J* 19(13):1845–1847.
- Lo T, et al. (2012) Phosphoproteomic analysis of human mesenchymal stromal cells during osteogenic differentiation. *J Proteome Res* 11(2):586–598.